

Remote sensing satellite formation for bistatic synthetic aperture radar observation

Marco D'Errico^{*a} and Antonio Moccia^{**b}

^aDipartimento di Ingegneria Aerospaziale; ^bDipartimento di Scienza e Ingegneria dello Spazio

ABSTRACT

In recent years the Italian Space Agency has been proceeding to the definition and launch of small missions. In this ambit, the BISSAT mission was proposed and selected along with five other missions for a competitive Phase A study. BISSAT mission concept consists in flying a passive SAR on board a small satellite, which observes the area illuminated by an active SAR, operating on an already existing large platform. Several scientific applications of bistatic measurements can be envisaged: improvement of image classification and pattern recognition, derivation of medium-resolution digital elevation models, velocity measurements, measurements of sea-wave spectra. BISSAT payload is developed on the basis of the X-band SAR of the COSMO/SkyMed mission, while BISSAT bus is based on an upgrade of MITA. Orbit design has been performed, leading to the same orbit parameters apart from the ascending node right ascension (5.24° shift) and the time of the passage on the ascending node (1.17s shift). A minimum distance at the passage of the orbit crossing point of about 42km (5.7s) is computed. To maintain adequate swath overlap along the orbit, attitude maneuver or antenna electronic steering must be envisaged and traded-off taking into account radar performance and cost of hardware upgrade.

Keywords: remote sensing satellite formation, bistatic synthetic aperture radar, mission analysis

1. INTRODUCTION

Separated transmitting and receiving antennas characterize bistatic radars. Since bistatic observation requires accurate time synchronization and antenna pointing between transmitter and receiver, it has been mainly applied by using one or both earth-based radar antennas. Furthermore, no sufficient attention has been given to the potential of using bistatic radar for large-scale earth observation. Whereas, several excellent numerical and experimental studies have been performed considering mainly complex targets of limited dimensions¹⁻². As a consequence, non-systematic overland bistatic measurements from aircraft or from spacecraft have been reported in literature³⁻⁵, in particular considering synthetic aperture radar (SAR). In spite of that, bistatic geometry from space platforms offers several key benefits.

After a description of scientific background in bistatic radar, with special emphasis on space based applications, this paper deals with orbit design of a bistatic SAR mission based on a small satellite (BISSAT) to be linked to Italian COSMO/SkyMed radar constellation. This study has been conducted within a competitive Phase A study issued by the Italian Space Agency to define the third Italian Small Scientific Mission. Proposed system envisages two antennas flying and operating in formation, along almost parallel orbits, for a two-year lifetime. It would be the first bistatic SAR implementation in space with two separate platforms.

2. SCIENCE BACKGROUND

A comprehensive analysis of bistatic radar can be found in 6-7. Basically, bistatic radar operates with separated transmitting and receiving antennas. Of course, the transmitting antenna can be monostatic, that is transmitting and receiving, and, consequently, it is possible to combine monostatic and bistatic data reflected by common covered areas or targets (Fig. 1). Bistatic data acquisition provides additional qualitative and quantitative measurements of surface microwave scattering properties. The main geometric parameters characterizing bistatic observations with respect to monostatic ones are the

* derrico@unina.it; phone +39 081 5010223; fax +39 081 5010285; Dipartimento di Ingegneria Aerospaziale - Seconda Università di Napoli, V. Roma 29, 81031 Aversa (CE), Italy; ** amoccia@unina.it; phone +39 081 7682158; fax +39 081 7682160; Dipartimento di Scienza e Ingegneria dello Spazio – Università di Napoli “Federico II”, P.le Tecchio 80, 80125 Napoli, Italy.

distance between the antennas (defined by using the baseline vector from transmitting to receiving antenna) and the transmitter-target-receiver angle (the bistatic angle) and plane (the bistatic plane).

Most of spaceborne active microwave missions have been carried out by monostatic radar. In the case of interferometry, when the two antennas operate simultaneously (i.e. non-repeat-track interferometry, Fig. 2), an antenna physical separation exists, but it must be kept within limited values, depending on wavelength, to avoid decorrelation and phase ambiguities⁸⁻⁹. Regarding applications of bistatic radar by making use of existing spaceborne systems, Pavelyev *et al.*¹⁰ explored refraction, absorption and scattering mechanisms in the atmosphere by means of a transmitting antenna onboard the orbital station Mir and a receiving antenna onboard a geo-synchronous satellite. Experiments have been conducted in planetology, by means of satellite-based transmitters and earth-based receivers¹¹⁻¹⁵ or a planet-based transmitter and a satellite-based receiver¹⁶. As an example, topography, reflectivity, scattering and root mean square slope have been computed for the surface of the moon, Mars and Venus. In these applications, bistatic radar has proven to be capable of providing information on surface texture and density at scales of few centimeters to a few hundred meters, along with highly accurate dielectric constant measurements. Moreover, remote probing in regions and under conditions not obtainable with Earth-based systems has been carried out. Recently, measurements of GPS (Global Positioning System) reflected signals for estimation of sea state and wind speed^{5, 17-18} and for remote sensing of rough surfaces¹⁹⁻²⁰ have been conducted.

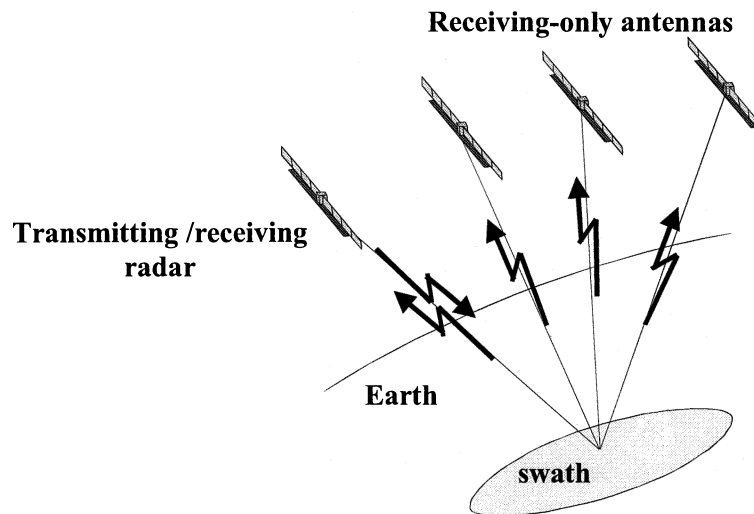


Figure 1: Schematic of spaceborne bistatic/multistatic radar

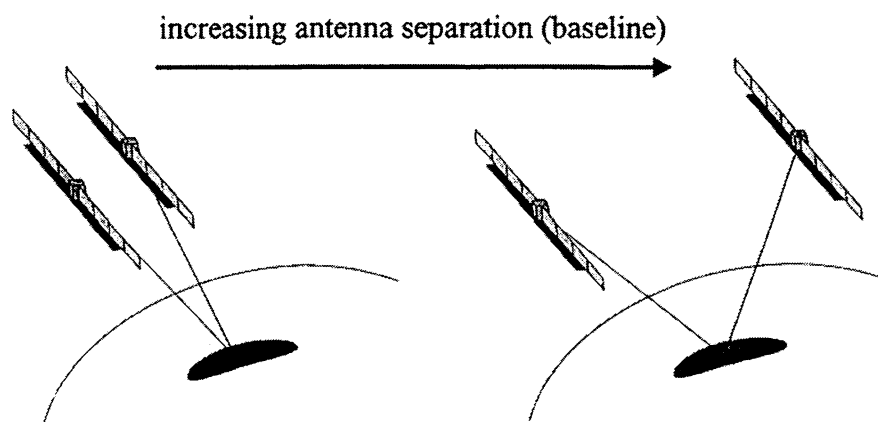


Figure 2: Schematic of spaceborne interferometric and bistatic observations

A limited number of spaceborne bistatic radar experiments has been proposed. Hsu and Lortz²¹ presented a first feasibility study of spaceborne bistatic radar aimed at worldwide surveillance. Guttrich and Sievers²², Ogronik *et al.*²³ and Hartnett and Davis²⁴ have analyzed integration of spaceborne radar illumination and bistatic reception by means of aerial vehicles for area surveillance and moving target detection. Regarding use of GPS reflected signals for bistatic remote sensing applications by means of spaceborne receivers, a constellation has been proposed²⁵, emphasizing sensors synchronization both in time and space. Bistatic radar altimeters for oceanographic applications have been studied²⁵⁻²⁷. A passive geosynchronous SAR system reusing backscattered digital audio broadcasting signals has been proposed²⁸ for volcanoes or coseismic motions monitoring or GPS corrections. Cherniakov *et al.*²⁹ recently studied a bistatic SAR based on non-cooperative LEO (Low Earth Orbit) commercial satellites for personal communications and an Earth-based receiver. Objective of the study was vessel detection at sea. Finally, a constellation of microsattellites mainly oriented to interferometry, therefore not really bistatic as far as applications are concerned, but equipped with low-cost, passive receivers, has been proposed³⁰⁻³¹.

This paper deals with a bistatic SAR based on a small satellite (BISSAT) to be linked to Italian COSMO-SkyMed and devoted to earth observation (Fig. 3). BISSAT is equipped with a receiving-only microwave system, that catches the echoes of the main monostatic X-band SAR (SAR2000). Within the innovative experiment, the two spacecraft will need accurate formation flying and next paragraph will point out key issues in orbit design.

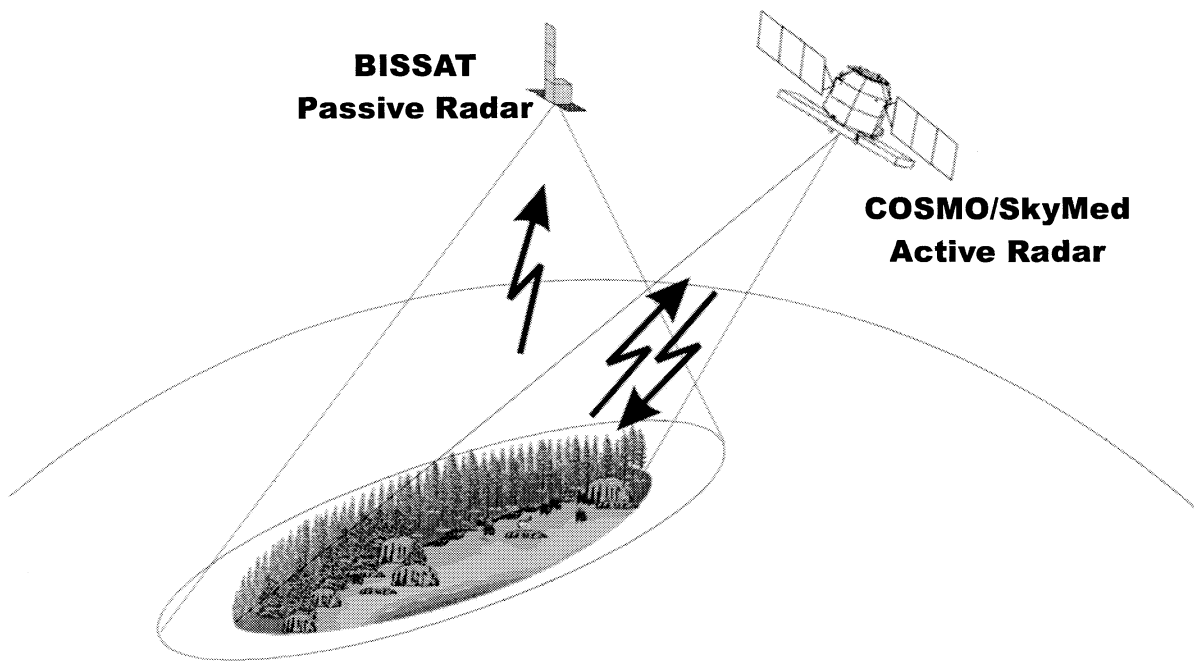


Figure 3: Schematic of proposed bistatic mission

3. ORBIT DESIGN FOR BISTATIC COVERAGE

The proposed bistatic mission consists of a receiving-only SAR (Synthetic Aperture Radar) which is designed to acquire the radar signal generated by a primary SAR and to be flown by a small satellite (BISSAT). Due to the mission time schedule envisaged by the Italian Space Agency (ASI), a radar satellite of the COSMO/SkyMed constellation has been selected as primary satellite. In particular, the radar segment of COSMO/SkyMed consists in a X-band SAR (SAR2000) whose main parameters are listed in Tab. 1. It is worth noting that SAR2000 has the capability of electronically steering the antenna beam along the elevation direction on the right with respect to the flight direction, which means that the elevation angle is negative if the sign's convention for attitude angles also holds for the antenna angles. As far as the receiving-only SAR (BISSAT2000) is concerned, it is based on SAR2000 design, but it is re-scaled (Tab. 1) in order to reduce volume, mass, power, and cost. The bus selected for flying BISSAT2000 is the MITA satellite, already developed under ASI sponsorship.

	SAR2000	BISSAT2000
Wavelength (cm)	3.125 (X-band)	3.125 (X-band)
Elevation angle (°)	23.3 ÷ 43.7	4
Azimuth angle (°)	NA	-3 ÷ 3
Antenna dimensions (m×m)	5.6 × 1.4	2.2 × 0.4
3dB aperture (°), elevation	1.1	3.9
3dB aperture (°), azimuth	0.28	0.72

Table 1: Main parameters of primary and passive radars

Orbit design is performed in order to guarantee the acquisition of bistatic radar data by means of the passive radar. To this end, BISSAT orbit must be designed according to the primary, active satellite one and under the assumptions that SAR2000 varies its off-nadir angle making use of its electronic steering capabilities. Since BISSAT has to fly in parallel with the active radar, its orbital parameters have to be accurately selected in order to guarantee the acquisition of the radar signal. As a consequence, the BISSAT orbit is designed with the same semi-major axis, eccentricity, and inclination of the primary mission, which guarantees the same precession rates (ascending node and perigee) for both orbits³²⁻³³. Moreover, both orbits are frozen by selecting the same argument of perigee³⁴. The difference between the two orbits is given by the ascending node right ascensions and by the times of the passages on the ascending node. In particular, the former is selected in order to guarantee a maximum range of latitudes where it is possible to acquire bistatic images. As far as the times of the passages on the ascending node are concerned, it is assumed that BISSAT, when it is on the equator, is also located in the elevation plane of SAR2000.

Orbit geometry is shown in Fig. 4. In particular, the intersections of orbit planes with spherical Earth will be referred to as orbital arcs, while the intersection of the radar elevation plane with the spherical Earth as elevation arc. The difference between the ascending node right ascensions is given by $\Delta\Omega$, while the difference between the time of the passages on the ascending node (Δt) corresponds to a shift in mean anomaly given by ΔM . Since the two orbits have the same orbit inclination (i), both their orbit arcs are tangent to the same parallel (the one at latitude $180^\circ - i$), but in different points. Moreover, the angle between the two orbit arcs in their intersection point is ψ . The angle along the orbit arc between the ascending node and the intersection of the orbit arcs is given by ξ (COSMO/SkyMed) and ζ (BISSAT).

It is worth noting that COSMO/SkyMed satellites perform a yaw attitude manoeuvre (yaw steering) in order to align the first body axis with the spacecraft-atmosphere velocity vector, which results in the reduction of the aerodynamic drag and in null Doppler centroid frequency in the monostatic radar images. The yaw attitude angle (γ) is a function of satellite anomaly (v) and angular velocity (ω), orbit inclination, and Earth angular velocity (Ω_\oplus) as follows:

$$\gamma = -\tan^{-1}\left(\frac{\sin i \cos v}{\omega / \Omega_\oplus - \cos i}\right) \quad (1)$$

From the spherical triangles in Fig. 4 it is possible to derive $\Delta\Omega$ and ΔM , provided that a relation between the radar off-nadir angle (ϑ) and the corresponding geocentric angle (ϑ_g) is found. Considering the triangle given by the centre of the Earth, the satellite actual position and the intersection of radar beam with spherical Earth we can derive the two functions $\vartheta_g(\vartheta)$ and $\vartheta(\vartheta_g)$ as follows:

$$\vartheta_g = \sin^{-1}\left[\frac{\sin \vartheta}{R_\oplus}\left(a \cos \vartheta - \sqrt{R_\oplus^2 - a^2 \sin^2 \vartheta}\right)\right] \quad (2)$$

$$\vartheta = \sin^{-1}\left\{\left[1 + \left(\frac{a / R_\oplus - \cos \vartheta_g}{\sin \vartheta_g}\right)^2\right]^{-1/2}\right\} \quad (3)$$

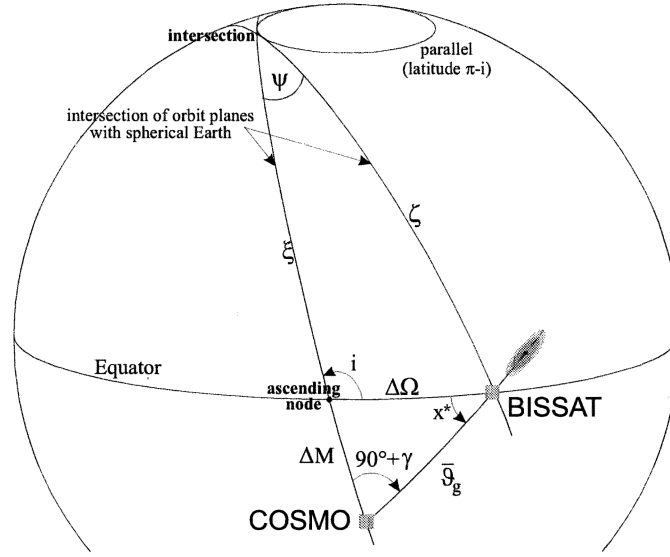


Figure 4: Geometry for orbit synchronisation

where a is the orbit semi-major axis and R_{\oplus} the Earth radius.

For the time being, let us assume that the elevation planes of the two radar swaths are aligned. If this is the case, considering that the transmitting/receiving (T/R) radar is pointed with an off-nadir angle $\vartheta_{T/R}$ and that the receiving-only (R/o) radar is mounted with a constant off-nadir angle $\vartheta_{R/o}$, if the two swath centres are to be coincident, it must be:

$$\bar{\vartheta}_g = \vartheta_g(\vartheta_{T/R}) - \vartheta_g(\vartheta_{R/o}) \quad (4)$$

Then, considering the perturbed mean motion³⁵, after some spherical trigonometry³⁶, $\Delta\Omega$ and Δt can be calculated as:

$$\Delta\Omega = \sin^{-1}\left(\frac{\sin\bar{\vartheta}_g \cos\gamma}{\sin i}\right) \quad (5)$$

$$\Delta M = \cos^{-1}\left(\frac{\cos\bar{\vartheta}_g \cos\Delta\Omega - \sin\Delta\Omega \cos i \sqrt{\sin^2\bar{\vartheta}_g - \sin^2\Delta\Omega \sin^2 i}}{1 - \sin^2\Delta\Omega \sin^2 i}\right) \quad (6)$$

$$\Delta t = \dot{M}\Delta M \quad (7)$$

Due to the dependence of γ on $360^\circ - \Delta M$ (Eq. 1), Eqs. 1.5÷1.7 must be solved by an iterative procedure.

Then, if elevation plane alignment is to be achieved, BISSAT satellite must be rotated of a yaw attitude angle $\gamma_{R/o,0}$:

$$\gamma_{R/o,0} = i - x^* - 90^\circ \quad (8)$$

$$x^* = \sin^{-1}\left(\frac{\sin\Delta M \sin i}{\sin\bar{\vartheta}_g}\right) \quad (9)$$

otherwise, the two swaths will be rotated around the BISSAT nadir of $\gamma_{R/o,0}$. But, it is also possible to vary the BISSAT antenna azimuth angle in order to move the BISSAT swath centre on the elevation arc of the T/R radar if swath relative rotation is acceptable.

Furthermore, the angles ψ , ξ , and ζ can be determined (Fig. 5) as:

$$\psi = \cos^{-1}(\sin^2 i \cos \Delta\Omega + \cos^2 i) \quad (10)$$

$$\xi = \sin^{-1}\left(\frac{\sin \Delta\Omega \sin i}{\sin \psi}\right) \quad (11)$$

$$\zeta = \pi - |\xi| \quad (12)$$

It is worth mentioning that: ϑ_g ranges between 0° and 90° for positive values of ϑ and between -90° and 0° whenever ϑ is negative; ϑ is always between 0° and 90° ; the sign of $\Delta\Omega$ is driven by the sign of $\bar{\vartheta}_g$; ψ ranges from 0° to 90° ; ξ is positive or negative, depending on the sign of $\Delta\Omega$; ζ ranges between 90° and 180° .

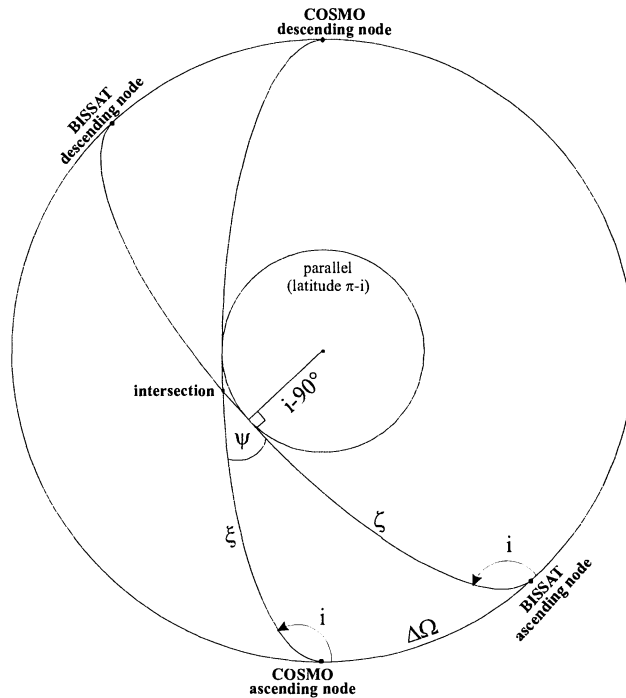


Figure 5: Orbit geometry – polar view

The model is applied making use of SAR2000 steering capability. In particular, since the distance between COSMO/SkyMed satellite and the area observed by the passive SAR decreases moving from the equator to the poles, it is straightforward to deduce that the required off-nadir angle will be a decreasing function of the latitude. Therefore, considering SAR2000 steering capability and in order to increase the range of latitudes where it is possible to acquire bistatic data, it is assumed that SAR2000 off-nadir angle achieves its maximum value when BISSAT is on the equator. Under this assumption, considering COSMO/SkyMed orbital parameters and steering capability, and remembering that BISSAT semi-major axis, eccentricity, and inclination coincide with the ones of SAR2000, the ascending node separation and the in-orbit separation can be computed (Tab. 2). Moreover, it is also possible to compute the yaw angle $\gamma_{R/0,0}$ ($\sim 3.84^\circ$), ψ ($\sim 5.2^\circ$), ξ ($\sim 89.6^\circ$), and ζ ($\sim 90.4^\circ$).

In addition, the orbit has been propagated in order to compute the distance between the two satellites (baseline) and to evaluate its variation along the orbit as a function of BISSAT anomaly (Fig. 6). In particular, the relative position of the BISSAT satellite with respect to COSMO/SkyMed satellite has been computed and projected to the orbiting right-handed reference frame fixed to the COSMO/SkyMed satellite (origin in the centre of mass, y-axis perpendicular to the orbital plane, z-axis directed along the local vertical towards Earth centre).

It is worth noting that: (1) B_x component ranges from 27.9km to 56.7km; (2) the absolute value of B_y component ranges

from 0 to 633.9km; (3) B_z ranges from 130m to 28.9km. Furthermore, the baseline is greater on the equator, where the satellites are at their maximum distance, whereas it attains its minimum value near the poles, where the two orbits intersect. Since B_y is almost null near the poles where B_z is also very small, B_x component represents the residual safety distance, as demonstrated by the fact that the minimum distance is about 42.67km, which is almost completely an along-orbit component (42.56km out of 42.67km). This distance corresponds to a time shift at the passage of the orbit crossing point of about 5.7s.

Semimajor axis (km)	6997.9
Inclination (°)	97.870
Eccentricity	0.00118
Argument of perigee (°)	90
Ascending node separation ($\Delta\Omega$, °)	5.2470
Anomaly separation (ΔM , °)	1.0663
Time separation (Δt , s)	17.255

Table 2: BISSAT orbit parameters

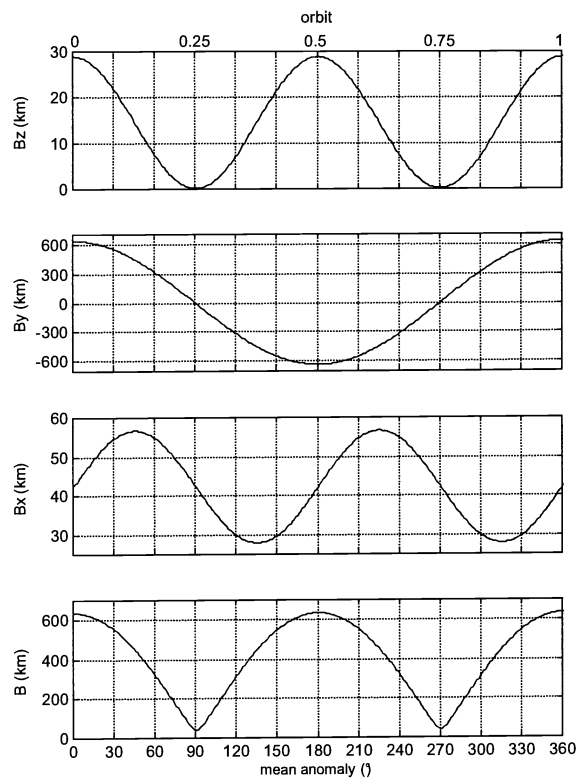


Figure 6: Satellite distance in the orbiting reference frame

4. CONCLUSIONS

The authors showed how the orbit of a satellite carrying a receiving-only SAR can be selected in order to catch the echoes backscattered from a target illuminated by an active radar able to steer the beam along the elevation direction. Considering figures and numerical results presented in the paper, it is a foregone conclusion that the bistatic configuration is lost as the

satellites rotates along their orbits. In particular, their across-orbit and along-orbit separations change along the orbit, which leads to lose swath superimposition. Furthermore, two main effects arise due to the variation of the yaw attitude angle of the primary satellite: (1) a relative rotation of the two radar swath and (2) an additional contribution to swath separation in the along-orbit direction.

These effects can be overcome by either attitude maneuvering the passive satellite or pointing the passive antenna or by an ad-hoc combination of the two techniques. In particular:

- across-orbit swath separation can be overcome by means of electronically steering the active radar antenna beam along the elevation direction;
- along-orbit swath separation can be nullified by electronically steering the passive antenna beam along the azimuth direction;
- swath relative rotation can be avoided if the passive satellite is yaw-rotated.

Trade-off can be made between radar payload / bus additional hardware implementation and mission performance to select the best option. In the proposed mission it is worth noting that:

- the first procedure makes use of the active radar (SAR2000) capability and does not require any upgrade in developed hardware;
- the second procedure is based on the use of passive radar (BISSAT2000) capability;
- the third procedure requires an upgrade of passive satellite bus (MITA) which is not currently capable of performing attitude rotation.

ACKNOWLEDGMENTS

This paper was carried out with financial funding of the Italian Space Agency.

REFERENCES

1. J.I. Glaser, 1989, "Some results in the bistatic radar cross section (RCS) of complex objects", *Proc. of the IEEE*, **77**, pp. 639-648.
2. R.L. Eigel, P.J. Collins, A.J. Terzuoli, G. Nesti, and J. Fortuny 2000, "Bistatic Scattering Characterization of Complex Objects", *IEEE Trans. on Geosc. and Rem. Sens.*, **38**, 5, pp. 2078-2092.
3. F.T. Ulaby, T.E. van Deventer, J.R. East, T.F. Haddock, and M.E. Coluzzi, 1988, "Millimeter-Wave Bistatic Scattering From Ground and Vegetated Targets", *IEEE Trans. on Geoscience and Remote Sensing*, **26**, 3, 229-243.
4. B. Hauck, F.T. Ulaby, and R.D. DeRoo, 1998, "Polarimetric Bistatic-Measurement Facility for Point and Distributed Targets", *IEEE Antennas and Propagation Mag.*, **40**, 1, 31-41.
5. A.K. Fung, C. Zuffada, and C.Y. Hsieh, 2001, "Incoherent Bistatic Scattering from the Sea Surface at L-Band", *IEEE Trans. on Geoscience and Remote Sensing*, **39**, 5, 1006-1012.
6. J.W. Caspers, 1970, "Bistatic and Multistatic Radar", in *Radar Handbook*, ed. by M.I. Skolnik, chapter 36, pp. 1-19, McGraw-Hill Inc., New York.
7. N.J. Willis, 1991, *Bistatic radar*, Artech House, Inc., Boston.
8. H.A. Zebker and J. Villasenor 1992, "Decorrelation in interferometric radar echoes", *IEEE Trans. on Geoscience and Remote Sensing*, **30**, 950-959.
9. Rosen, P.A., Hensley, S., Joughin, I.R., Li, F.K., Madsen, S.N., Rodriguez, E., and Goldstein, R.M., 2000, "Synthetic Aperture Radar Interferometry", *Proc. of the IEEE*, **88**, 3, 333-382.
10. Pavelyev, A.G., Volkov, A.V., Zakharov, A.I., Krutikh, S.A., and Kucherjavenkov, A.I., 1996, "Bistatic Radar as a tool for earth investigation using small satellites", *Acta Astronautica*, **39**, 721-730.
11. Parker, M.N., and Tyler, G.L., 1973, "Bistatic-radar estimation of surface-slope probability distributions with applications to the moon", *Radio Science*, **8**, 3, 177-184.
12. Tyler, G.L., and Howard, H.T., 1973, "Dual-Frequency Bistatic-Radar Investigations of the Moon with Apollos 14 and 15", *J. of Geophysical Research*, **78**, 23, 4852-4874.
13. Simpson, R.A., 1993, "Spacecraft Studies of Planetary Surfaces Using Bistatic Radar", *IEEE Trans. on Geoscience and Remote Sensing*, **31**, 2, 465-482.

14. Simpson, R.A., and Tyler, G.L., 1982, "Radar Scattering Laws for the Lunar Surface", *IEEE Trans. on Antennas and Propagation*, **30**, 3, 438-449.
15. Simpson, R.A., and Tyler, G.L., 1999, "Reanalysis of Clementine bistatic radar data from the lunar South Pole", *J. of Geophysical Research*, **104**, E2, 3845-3862.
16. Tang, C.H., Boak, T.I.S., and Grossi, M.D., 1977, "Bistatic radar measurement of electrical properties of the martian surface", *J. of Geophysical Research*, **82**, 4305-4315.
17. Zavorotny, V.U., Voronovich, A.G., Katzberg, S.J., Garrison, J.L., and Komjathy, A., 2000, "Extraction of Sea State and Wind Speed from Reflected GPS Signals: Modeling and Aircraft Measurements", *Proc. of IGARSS '00*.
18. Martín-Neira, M., Caparrini, M., Font-Rossello, J., Lannelongue, S., and Serra Vallmitjana, C., 2001, "The PARIS Concept, An Experimental Demonstration of Sea Surface Altimetry Using GPS Reflected Signals", *IEEE Trans. on Geoscience and Remote Sensing*, **39**, 1, 142-150.
19. Zahn, D., and Sarabandi, K., 2000, "Simulation of Bistatic Scattering For Assessing the Application of Existing Communication Satellites to Remote Sensing of Rough Surfaces", *Proc. of IGARSS '00*, 1528-1530.
20. Zavorotny, V.U., and Voronovich, A.G., 2000, "Bistatic GPS Signal Reflections at Various Polarizations from Rough Land Surface with Moisture Content", *Proc. of IGARSS '00*.
21. Hsu, Y.S., and Lortz, D.C., 1986, "Spaceborne bistatic radar - an overview", *IEE Proc.-F*, **133**, 642-648.
22. Guttrich, G.L., and Sievers, W.E., 1997, "Wide Area Surveillance Concepts Based on Geosynchronous Illumination and Bistatic UAV or Satellite Reception", *IEEE Aerospace Conf. Proc.*, **2**, 171-180.
23. Ogrodnik, R.F., Wolf, W.E., Schneible, R., and McNamara, J., 1997, "Bistatic Variants of Spacebased Radar", *IEEE Aerospace Conf. Proc.*, **2**, 159-169.
24. Hartnett, M.P., and Davis, M.E., 2001, "Bistatic Surveillance Concept of Operations", *Proc. of the 2001 IEEE Radar Conf.*, 75-80.
25. Martín-Neira, M., Mavrocordatos, C., and Colzi, E., 1998, "Study of a Constellation of Bistatic Radar Altimeters for Mesoscale Ocean Applications", *IEEE Trans. on Geoscience and Remote Sensing*, **36**, 6, 1898-1904.
26. Picardi, G., Seu, R., Sorge, S.G., and Martín-Neira, M., 1998, "Bistatic Model of Ocean Scattering", *IEEE Trans. on Antennas and Propagation*, **46**, 10, 1531-1541.
27. Alberti, G., and Zelli, C., 1999, "Design of Bistatic Altimetric Mission for Oceanographic Applications", *Space Technology*, **19**, 2, 83-96.
28. Prati, C., Rocca, F., Giancola, D., and Monti Guarnieri, A., 1998, "Passive Geosynchronous SAR System Reusing Backscattered Digital Audio Broadcasting Signals", *IEEE Trans. on Geoscience and Remote Sensing*, **36**, 6, 1973-1976.
29. Cherniakov, M., Kubik, K., and Nezhlin, D., 2000, "Bistatic Synthetic Aperture Radar with Non-Cooperative LEOS Based Transmitter", *Proc. of IGARSS '00*, 861-862.
30. Massonnet, D., 2001, "Capabilities and Limitations of the Interferometric Cartwheel", *IEEE Trans. on Geoscience and Remote Sensing*, **39**, 3, 506-520.
31. Massonnet, D., 2001, "The interferometric cartwheel: a constellation of passive satellites to produce radar images to be coherently combined", *Int. J. of Remote Sensing*, **22**, 12, 2413-2430.
32. Duck, K.I., and J.C. King, 1983. "Orbital Mechanics for Remote Sensing", in *Manual of Remote Sensing* (2nd ed.), ed. by R.N. Colwell, Chapter 16 - Vol. 1, American Society of Photogrammetry, Falls Church, Virginia.
33. Kozai, Y., 1959. "The Motion of a Close Earth Satellite", *The Astronomical Journal*, **64**, pp. 367-377.
34. Chobotov, V.A., (Editor), 1991. *Orbital Mechanics*, American Institute of Aeronautics and Astronautics, Washington, DC, pp. 365.
35. Brooks, D.R., 1977. "An Introduction to Orbit Dynamics and Its Application to Satellite-Based Earth Monitoring Mission", NASA RP-1009, Washington, DC.
36. Wertz, R.W. (editor), 1978. *Spacecraft Attitude Determination and Control*, Kluwer Academic Publishers, Boston, MA, pp. 858.